










Periodic repeating fast radio bursts: interaction between a magnetized neutron star and its planet in an eccentric orbit

ABDUSATTAR KURBAN (阿布都沙塔尔·库尔班) ^{1,2,3,4} YONG-FENG HUANG (黄永锋) ^{2,5} JIN-JUN GENG (耿金军) ⁶
BING LI (李兵) ^{7,8} FAN XU (许帆) ² XU WANG (王旭) ² XIA ZHOU (周霞) ^{1,3,4}
ALI ESAMDIN (艾力·伊沙木丁) ¹ AND NA WANG (王娜) ^{1,3,4}

¹*Xinjiang Astronomical Observatory, Chinese Academy of Sciences, Urumqi 830011, Xinjiang, People's Republic of China*

²*School of Astronomy and Space Science, Nanjing University, Nanjing 210023, People's Republic of China*

³*Key Laboratory of Radio Astronomy, Chinese Academy of Sciences, Urumqi 830011, Xinjiang, People's Republic of China*

⁴*Xinjiang Key Laboratory of Radio Astrophysics, Urumqi 830011, Xinjiang, People's Republic of China*

⁵*Key Laboratory of Modern Astronomy and Astrophysics (Nanjing University), Ministry of Education, Nanjing 210023, People's Republic of China*

⁶*Purple Mountain Observatory, Chinese Academy of Sciences, Nanjing 210023, People's Republic of China*

⁷*Key Laboratory of Particle Astrophysics, Chinese Academy of Sciences, Beijing 100049, People's Republic of China*

⁸*Particle Astrophysics Division, Institute of High Energy Physics, Chinese Academy of Sciences, Beijing 100049, People's Republic of China*

ABSTRACT

Fast radio bursts (FRBs) are mysterious transient phenomena. The study of repeating FRBs may provide useful information about their nature due to their redetectability. The two most famous repeating sources are FRBs 121102 and 180916, with a period of 157 days and 16.35 days, respectively. Previous studies suggest that the periodicity of FRBs is likely associated with neutron star (NS) binary systems. Here we introduce a new model which proposes that periodic repeating FRBs are due to the interaction of a NS with its planet in a highly elliptical orbit. The periastron of the planet is very close to the NS so that it would be partially disrupted by tidal force every time it passes through the periastron. Fragments generated in the process could interact with the compact star through the Alfvén wing mechanism and produce FRBs. The model can naturally explain the repeatability of FRBs with a period ranging from a few days to several hundred days, but it generally requires that the eccentricity of the planet's orbit should be large enough. Taking FRBs 121102 and 180916 as examples, it is shown that the main features of the observed repeating behaviors can be satisfactorily accounted for.

Keywords: Radio transient sources (2008); Neutron stars (1108); Exoplanets (498); Tidal disruption (1696)

1. INTRODUCTION

The first discovery of fast radio bursts (FRBs) by Lorimer et al. (2007) and consequent reports of five similar sources by Keane et al. (2012) and Thornton et al. (2013) opened a new window in astronomy. Since then FRBs have become an active topic for research. The isotropic energy released by FRBs is in the range of $10^{38} - 10^{46}$ erg, and their duration is typically several milliseconds. The observed dispersion measure is $\sim 110 - 2596$ pc cm⁻³ (Petroff et al. 2019), which strongly hints that FRBs are of cosmological origin. According to the observed repeatability (Petroff et al. 2015), these enigmatic events may come from two kinds of progenitors, i.e. repeating sources and nonrepeating sources.

Many models (see Platts et al. (2019) for a recent review) have been proposed to interpret the properties of FRBs. However, their underlying physics – the progenitor as well as emission mechanism – remains unclear (Katz 2018;

Petroff et al. 2019; Platts et al. 2019; Cordes & Chatterjee 2019; Zhang 2020). Repeating FRBs, in particular periodic repeating FRBs, may provide valuable information about the nature of this mysterious phenomenon.

Here we will mainly focus on the periodic repeating activities of FRBs. The most famous periodic repeating sources are FRB 121102 and FRB 180916. FRB 121102 has a period of 157 days (Rajwade et al. 2020), and FRB 180916 has a period of 16.35 days (Chime/Frb Collaboration et al. 2020). Two kinds of models, the single-star model and binary model, have been proposed to interpret the periodic repeatability of these FRBs. The single-star models are mainly concerned with the precession of neutron stars (NS) (Levin et al. 2020; Yang & Zou 2020; Sob'yanin 2020; Zanazzi & Lai 2020) while the binary models associate FRBs with the interaction between the two objects in NS binary systems (Mottez & Zarka 2014; Dai et al. 2016; Zhang 2017, 2018; Lyutikov et al. 2020; Ioka & Zhang 2020; Dai & Zhong 2020; Dai 2020; Gu et al. 2020; Mottez et al. 2020; Geng et al. 2020; Decoene et al. 2021; Du et al. 2021). Usually, the precession period of NS is unlikely to be as long as 16.35 days (Chime/Frb Collaboration et al. 2020). Additionally, the fixed emission region of FRBs in the precession models has not yet been properly addressed (Xiao et al. 2021). Various observational facts imply that binary models are more likely favored by the periodicity of FRBs. The binary-interaction models can be further categorized into two main classes: wind-like models and accretion/collision-like models. The wind-like models include the binary comb mechanism (Zhang 2017, 2018; Ioka & Zhang 2020), mild pulsars in tight O/B-star binaries (Lyutikov et al. 2020), small bodies orbiting around a pulsar or a magnetar (Mottez & Zarka 2014; Mottez et al. 2020; Voisin et al. 2021), and Kozai-Lidov feeding of NSs in binary systems (Decoene et al. 2021). The collision/accretion-like models include the collision between a magnetized NS and an asteroid belt (Dai et al. 2016; Smallwood et al. 2019; Dai & Zhong 2020; Dai 2020), accretion of strange stars from low-mass companion stars (Geng et al. 2021), and NS-white dwarf (WD) interactions (Gu et al. 2016, 2020). FRBs and their counterparts in other wavelengths have been studied by Yang & Zhang (2021), Yang (2021), and by many other authors. As suggested earlier by a few authors, collisions between small bodies and a NS can generate transient events such as gamma-ray bursts (Campana et al. 2011), glitch/anti-glitches and X-ray bursts (Huang & Geng 2014; Yu & Huang 2016), and FRBs (Geng & Huang 2015; Dai et al. 2016).

Tidal disruption of minor planets/asteroids around WDs has also been extensively studied (Bear & Soker 2013; Vanderburg et al. 2015; Granvik et al. 2016). Recent simulations (Malamud & Perets 2020a,b) have shown that a planet in a highly eccentric orbit around a WD could be tidally disrupted by tidal force, and materials in the inner side of the orbit would be accreted by the WD. Accreted clumps of such materials may be responsible for the pollution of a WD's atmosphere by heavy elements (Vanderburg et al. 2015; Malamud & Perets 2020a,b). Similar processes (disruption of a planet) can also occur in NS-planet systems if the initial parameters of the planetary system fulfill the tidal disruption condition (Brook et al. 2014). In fact, GRB 101225A may occur in this way (Campana et al. 2011). Much efforts have also been made to search for close-in exoplanets around pulsars (Geng & Huang 2015; Huang & Yu 2017; Kuerban et al. 2020).

In this study, we propose a new model to explain the periodic repeating properties of FRB sources. We argue that when a planet is in a highly eccentric orbit around a NS, it would be partially disrupted every time it passes through the pericenter. The major fragments generated during the disruption will interact with the pulsar (rotating NS) wind to produce a series of FRBs. This model can naturally explain the periodic behavior of repeating FRBs. The structure of our paper is as follows. In Section 2, we present the basic framework of our model for repeating FRBs. In Section 3, the wind-clump interaction mechanism for FRBs is introduced. In Section 4, the periodicity and active window are described in view of the model. In Section 5, we estimate the evaporation timescale for a planet in an elliptical orbit. In Section 6, we address the possible existence of pulsar planets in highly eccentric orbits. Finally, Section 7 presents our conclusions and some brief discussion.

2. MODEL

The planet-disruption interpretation for the pollution of a WD's atmosphere by heavy elements (Vanderburg et al. 2015; Granvik et al. 2016; Stephan et al. 2017; Malamud & Perets 2020a,b) and the Alfvén wing theory for FRBs (Mottez & Zarka 2014; Mottez et al. 2020) motivates us to investigate the periodic repeating activities of FRBs in the framework of a NS-planet interaction model. When a planet is in an highly elliptical orbit with the periastron distance being small enough, it might be partially disrupted every time it passes through the pericenter. The disrupted fragments formed during this process will regularly interact with the host NS and produce periodic repeating FRBs.

Figure 1 illustrates the general picture of a NS-planet system in an eccentric orbit. We assume that the central star is a NS with a mass $M_\star = 1.4 M_\odot$, and the companion is a rocky planet with a mass m , mean density $\bar{\rho}$, and an orbital

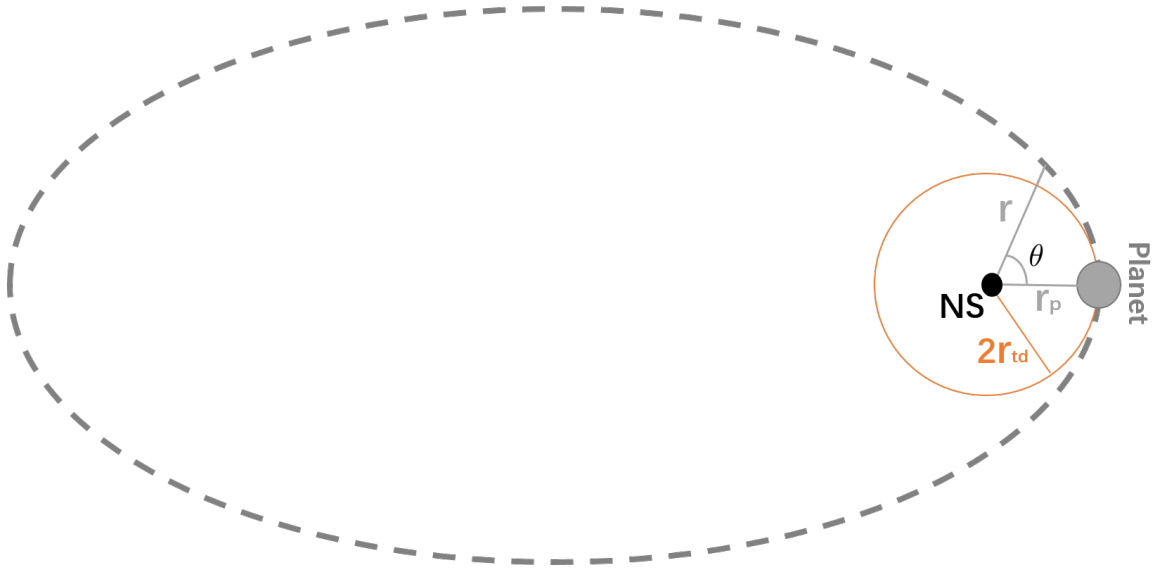


Figure 1. Schematic illustration (not to scale) of a pulsar planet in a highly eccentric orbit. The central star is a NS and the planet is assumed to be a typical rocky object. r is the separation between the NS and the planet at phase θ . r_p is the periastron distance of the orbit. $2r_{\text{td}}$ is a characteristic distance at which partial tidal disruption will occur (see text for more details).

period P_{orb} . The semi-major axis (a) and orbital period are related by the Kepler's third law as

$$\frac{P_{\text{orb}}^2}{a^3} = \frac{4\pi^2}{G(M_\star + m)}. \quad (1)$$

The distance between the NS and planet at phase θ (the true anomaly; see Figure 1) in the eccentric orbit is

$$r = \frac{a(1 - e^2)}{1 + e \cos \theta}, \quad (2)$$

where e is the eccentricity of the orbit. The characteristic tidal disruption radius of the planet depends on its density as (Hills 1975)

$$r_{\text{td}} \approx \left(\frac{6M_\star}{\pi \bar{\rho}} \right)^{1/3}. \quad (3)$$

Whether a planet will be tidally disrupted or not depends on its separation (r) with respect to the NS. If r is smaller than a critical value of $2.7r_{\text{td}}$, then it will begin to be partially disrupted (Liu et al. 2013). The separation between the planet and NS is different when the planet is at different orbital phase. At periastron, it is

$$r_p = a(1 - e). \quad (4)$$

For a highly elliptical orbit on which the separation varies in a very wide range, the planet may be tidally affected mainly near the periastron and it is relatively safe at other orbital phases. Here, we focus on the disruption near the periastron. If the orbit is too compact (for example, $r_p \leq r_{\text{td}}$), then the disruption is violent and the planet will be completely destroyed. However, when $r_{\text{td}} < r_p < 2.7r_{\text{td}}$, then the planet will only be partially disrupted every time it passes by the periastron. Since the density at the surface is relatively small, the outer crust of the planet will be destroyed first, which gives birth to a number of fragments with the size of a few kilometers. The main portion of the planet will retain its integrity. The idea of partial disruption has been supported both from observations (Manser et al. 2019) and simulations (Liu et al. 2013; Malamud & Perets 2020a,b).

In our study, we assume $r_p = 2r_{\text{td}}$ for simplicity, which satisfies the condition for a partial disruption. We can then calculate the relation between the periastron distance and the orbital period, which depends on the orbital eccentricity. The results are shown in Figure 2. For comparison, we have also marked the partial tidal disruption distance ($2r_{\text{td}}$

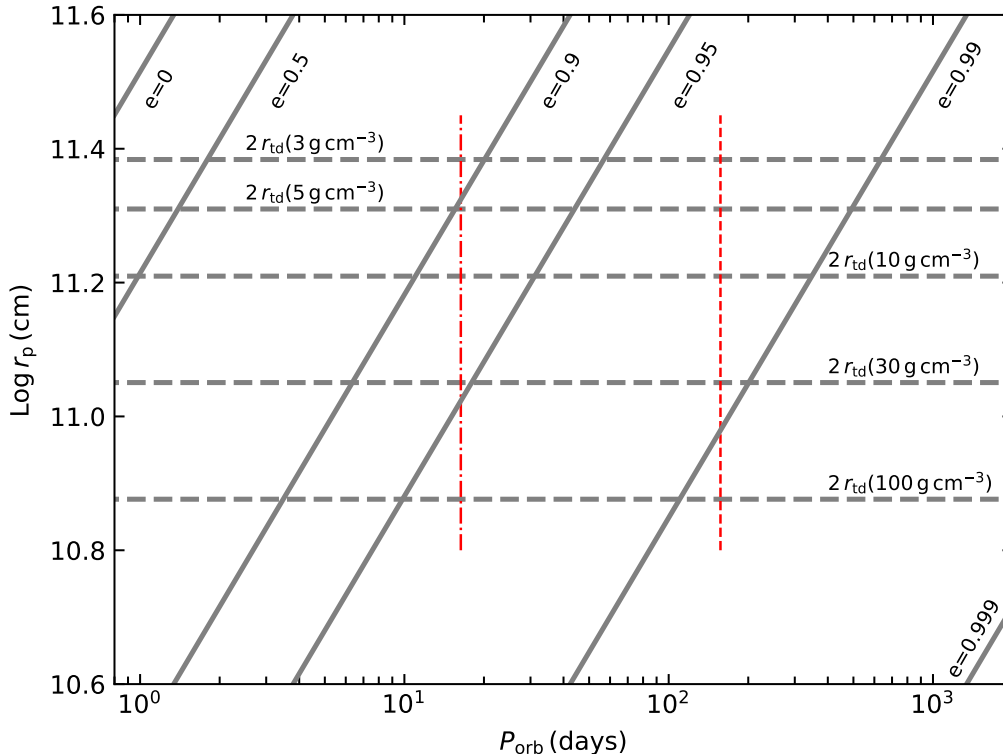


Figure 2. The periastron distance as a function of the orbital period for various eccentricities. Horizontal lines correspond to $r_p = 2r_{td}$ for different planet densities (marked in the brackets). The dashed-dotted vertical line corresponds to an orbital period of 16.35 days, and the dashed vertical line is 157 days.

for the planet with a particular density) as horizontal lines. We can see that a partial disruption would occur near the periastron for a wide range of orbital periods. For example, for an orbit with $e = 0.95$, the partially disrupted planet will have an orbital period of ~ 20 days when its mean density is 30 g cm^{-3} . If the mean density is 10 g cm^{-3} , 5 g cm^{-3} , or 3 g cm^{-3} , then the orbital period will be 30 days, 43 days, and 60 days, correspondingly. More generally, for a planet with a mean density ranging from 3 to 10 g cm^{-3} , partial disruption will occur for $P_{orb} \sim 2 - 600$ days when the eccentricity is $e \sim 0.5 - 0.99$. Note that the mass of the planet does not affect the disruption too much. The disruption process is mainly determined by orbital parameters and the mean density of the planet.

A number of fragments will be generated during the partial disruption process. These fragments will experience some complicated dynamical interactions such as gravitational perturbation (Naoz (2016), see below) and scattering/collision (Cordes & Shannon 2008). These interactions lead the clumps to orbit around the central NS with slightly different orbital parameters (velocity, semi-major axis, eccentricity, inclination relative to the planet’s orbit, etc.). In the orbiting process, the interaction between the clumps and the pulsar wind can generate FRBs through the Alfvén wing mechanism (Mottez & Zarka 2014; Mottez et al. 2020).

The above process of partial disruption happens periodically every time the surviving main portion of the planet passes through the periastron. Consequently, this regular interaction can account for the periodic repeating FRBs.

3. WIND-CLUMP INTERACTION MECHANISM

Orbiting small bodies immersed in the relativistic wind of a highly magnetized pulsar can be the sources of repeating FRBs (Mottez & Zarka 2014; Mottez et al. 2020). The interaction between the small body and the pulsar wind produces a small Alfvén wing angle (see Table 1 in Mottez & Zarka (2014)). When the wind plasma crosses the Alfvén wing, it sees a rotation of the ambient magnetic field that can cause radio wave instabilities. In the observer’s reference frame, the radiation is focused into a very small solid angle due to the relativistic beaming effect, which amplifies the flux

density and produces FRBs. At a distance of ~ 1 AU from the pulsar, the required size for a small body to produce FRBs is a few kilometers.

When a pulsar with a surface magnetic field B_\star and angular frequency Ω_\star interacts with a small body of size R_c , it generates an Alfvén wing with a power of (Mottez & Heyvaerts 2020)

$$\dot{E}_A = \frac{\pi}{\mu_0 c^3} B_\star^2 R_\star^6 \Omega_\star^4 R_c^2 r^{-2}, \quad (5)$$

where μ_0 is the magnetic conductivity, c is the speed of light, R_\star is the radius of the pulsar, r is the separation between the two objects and is a function of θ as shown in Eq. (2). The radio emission power of the Alfvén wing is

$$\dot{E}_{\text{radio}} = \epsilon_r \dot{E}_A, \quad (6)$$

where $2 \times 10^{-3} \leq \epsilon_r \leq 10^{-2}$ is the radiation efficiency (Zarka et al. 2001; Zarka 2007). In the observer’s reference frame, the radio flux density generated from the interaction between the pulsar wind and a small sized object is (Mottez et al. 2020)

$$\left(\frac{S}{\text{Jy}}\right) = 2.7 \times 10^{-9} A_{\text{cone}} \left(\frac{\gamma}{10^5}\right)^2 \left(\frac{\epsilon_r}{10^{-3}}\right) \left(\frac{R_c}{10^9 \text{cm}}\right)^2 \left(\frac{r}{\text{AU}}\right)^{-2} \left(\frac{R_\star}{10^6 \text{cm}}\right)^6 \left(\frac{B_\star}{10^9 \text{G}}\right)^2 \left(\frac{P_\star}{10^{-2} \text{s}}\right)^{-4} \left(\frac{D}{1 \text{Gpc}}\right)^{-2} \left(\frac{\Delta\nu}{1 \text{GHz}}\right)^{-1}, \quad (7)$$

where γ is the Lorentz factor of the pulsar wind, $\Delta\nu$ is the emission bandwidth, D is the luminosity distance, P_\star is the spin period of the pulsar. In Eq. (7), $A_{\text{cone}} = 4\pi/\Omega_A$ is an indication of the beaming factor. The radio waves are emitted into a solid angle Ω_A in the source frame, which could be nearly isotropic. Note, however, that the radiation is limited in a solid angle $(\Omega_A/4)\gamma^{-2}$ in the observer’s reference frame due to the beaming effect; the observer can see the FRBs only when the radio beams point toward the observer.

As described in Section 2, the orbits of the disrupted clumps will change due to dynamical interactions. Here, for simplicity, when studying their interaction with the pulsar wind, we only consider their first round of motion in the orbit. We further assume that the orbit is similar to that of the original planet. Using the orbital parameters constrained from the partial disruption condition, we can estimate the peak flux of the FRB generated due to the interaction of a clump and the pulsar wind through Eq. (7). As an example, we have applied our model to FRBs 180916 and 121102. In our calculations, we take $\Omega_A = 0.1$ sr, $\gamma = 3 \times 10^6$, and $\epsilon_r = 10^{-2}$. Figure 3 shows the flux variation versus the orbital phase, which is caused by the variation of the distance r between the NS and the clump due to the large orbital eccentricity. Panel (a) of Figure 3 shows the effect of P_{orb} on the flux density. It is clear that the flux density is quite insensitive to P_{orb} under the partial disruption condition. Panels (b) – (d) of Figure 3 show the effects of B_\star and R_c on S for fixed P_{orb} and P_\star . From these plots we can see that the effects of B_\star and R_c are significant. Note that for many parameter sets, S is larger than the detection threshold (0.3 Jy) during a significant portion of the orbital phase.

In a typical duty circle, the observed FRB number is of the order of a few. This indicates that usually only a few major fragments are generated during the passage of the periastron. For the clump-wind interaction mechanism, the required size of the small body that can produce FRBs is a few kilometers. It is quite typical for the fragments generated during a partial disruption. Simulations show that the tidal disruption of a planet by a compact star such as a WD can give birth to fragments ranging from a few kilometers to ~ 100 km (Malamud & Perets 2020a,b). This is interesting to note that the number of observed bursts is related with fluence as $N \propto F^{\alpha+1}$, where $\alpha = -2.3 \pm 0.3$ for FRB 180916 (Chime/Frb Collaboration et al. 2020). So, there are many more low-fluence FRBs as compared with high-fluence ones. This is consistent with our NS-planet interaction model. In the partial disruption process, the number of smaller clumps is usually larger than that of bigger fragments (Malamud & Perets 2020a,b).

4. PERIODICITY AND ACTIVE WINDOW

4.1. Periodicity

Observations indicate that FRB 180916 seems to have a repeating period of 16.35 days (Chime/Frb Collaboration et al. 2020), while FRB 121102 may have a period of 157 days (Rajwade et al. 2020). This suggests that the periods of repeating FRBs may vary in a relatively wide range. In our model, the period is mainly determined by the orbital motion of the planet. The observed periods thus exert some constraints on the parameters of our NS-planet systems. Here we show that the planet-disruption model can meet the observational requirements.

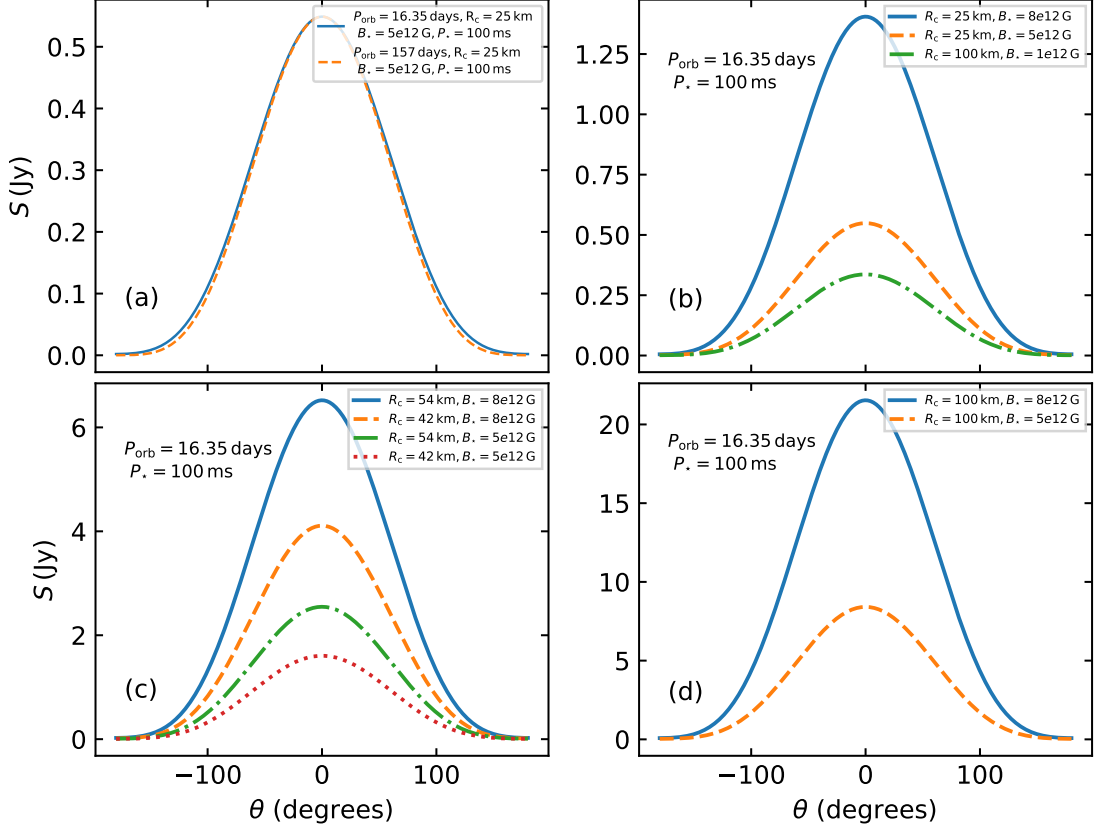


Figure 3. The flux density of FRBs vs. the orbital phase. The orbital parameters are taken by considering the partial disruption condition. Panel (a) shows the effect of the orbital period on the flux density. Panels (b), (c), and (d) show the effects of the surface magnetic field and the clump size on the flux density.

As mentioned in Section 2, we take $r_p = 2r_{td}$ as the typical case for the partial disruption condition. This naturally leads to a relation of

$$a(1-e) = 2 \left(\frac{6M_*}{\pi \bar{\rho}} \right)^{1/3}. \quad (8)$$

Combining Eq. (1) and Eq. (8), one can derive the relationship between various parameters of the NS-planet systems. In Figure 4, we have plot the relation between the eccentricity and orbital period for planets that satisfy the partial disruption condition. The calculations are conducted for planets with a mean density of $\bar{\rho} = 3 \text{ g cm}^{-3}$, 5 g cm^{-3} , and 10 g cm^{-3} , respectively. We can see that with an increase of the period, the eccentricity should also increase. This is easy to understand. The key point is that the periastron distance ($r_p = 2r_{td}$) is almost fixed by the mean density in our framework. At the same time, to acquire a long orbital period, the semi-major axis should be large enough. As a result, the eccentricity will have to be large. From Figure 4, we can see that to get a period of ~ 1 day, an eccentricity of $e \sim 0.3 - 0.5$ is enough. However, to achieve a period of ~ 16 days, $e \sim 0.9$ will be required, while for $P_{orb} \geq 160$ days, $e \geq 0.97$ is necessary. In general, Figure 4 demonstrates that partial disruption does can happen periodically under proper conditions, and repeating FRBs with periods ranging from ~ 1 to ~ 1000 days are possible.

4.2. Active window

In the context of the Alfvén wing mechanism, the active window of FRBs is determined by the distribution of clumps in the orbit. The clumps originating from different parts of the planet have slightly different orbital parameters. The semi-major axis of the clumps disrupted from a planet around a WD is given in Malamud & Perets (2020a). Here, we

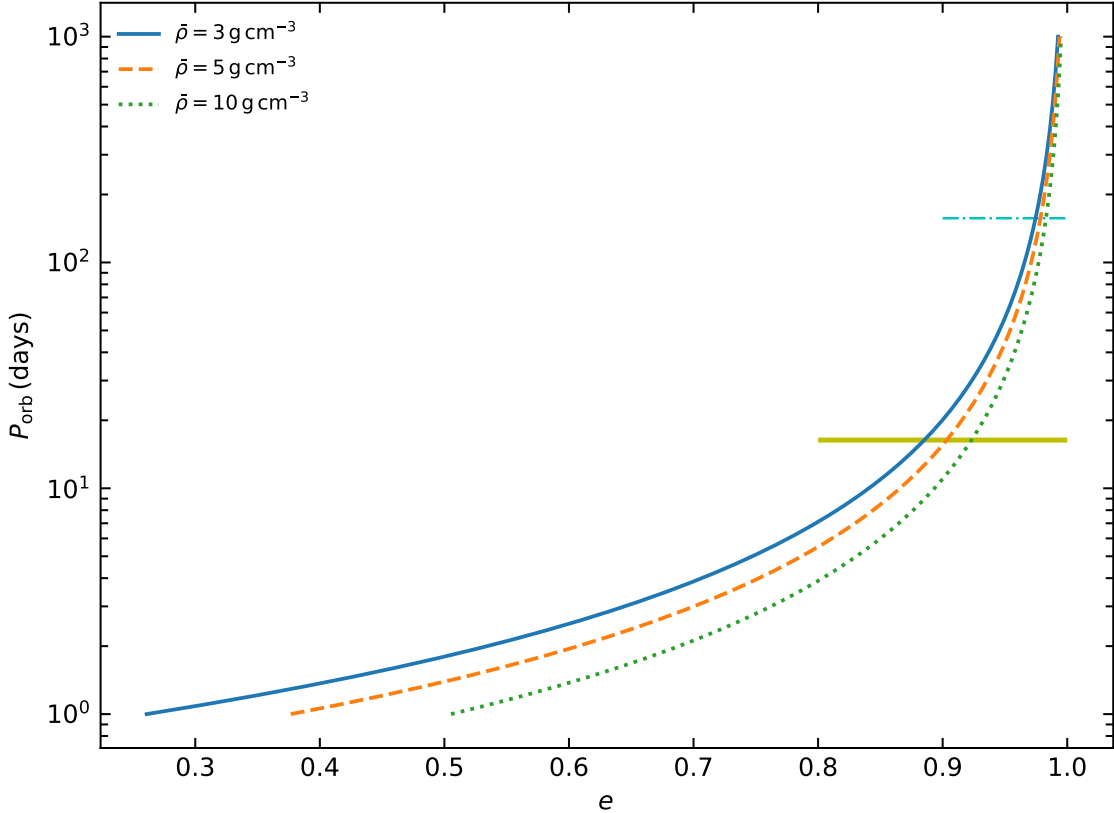


Figure 4. Orbital period as a function of the eccentricity under the partial tidal disruption condition $r_p = 2 r_{td}$. The calculation is conducted for three different densities. The two horizontal short lines represent orbital periods of 16.35 days and 157 days, respectively.

applied it to our model as

$$a' = \begin{cases} a \left(1 + a \frac{2R}{d(d-R)}\right)^{-1}, & \text{(In the direction of NS)} \\ a \left(1 - a \frac{2R}{d(d+R)}\right)^{-1}, & \text{(In the opposite direction of NS)} \end{cases} \quad (9)$$

where a is still the planet's original semi-major axis, d is the distance between the pulsar and planet at the moment of breakup, and R is the displacement of the clump relative to the planet's mass center at the moment of breakup ($R = 0$ corresponds to the center of the planet). In the opposite direction of the NS, there is a critical displacement $R_{crit} = d^2/(2a - d)$. Particles with $R < R_{crit}$ are bound while particles with $R > R_{crit}$ are unbound to the planet (Malamud & Perets 2020a).

The semi-major axes of disrupted clumps are different since their displacements (R) are different (see Eq. (9)). Hence, their velocities and orbital periods are also different. The orbital velocity can be calculated by $v = r\omega$, where $\omega = (2\pi/P_{orb})(1 + e \cos \theta)^2/(1 - e^2)^{3/2}$ (Sepinsky et al. 2007). Substituting r with Eq. (2), we get

$$v^2 = \frac{G(M_\star + m)}{a} \frac{(1 + e \cos \theta)^2}{(1 - e^2)}. \quad (10)$$

This is the velocity of the planet at phase θ . We can further obtain the velocity of the disrupted clumps by substituting a in Eq. (10) with a' of Eq. (9).

The active window of the wind interaction mechanism is determined by the difference of the orbital periods of the clumps in the innermost and outermost orbits, which themselves can be obtained by combining Eq. (9) and Eq. (1). Here, we assume that the line of sight lies in the orbital plane. In our calculations, for simplicity, we assume that the

clumps are disrupted from the surface of the planet (i.e. $R = R_c = (3m/4\pi\bar{\rho})^{1/3}$) at the periastron $d = r_p = 2r_{td}$. As an example, we take a planet's parameters as $P_{\text{orb}} = 100$ days, $m = 10^{-6} M_{\odot}$, and $\bar{\rho} = 5 \text{ g cm}^{-3}$ (correspondingly, $e = 0.971$). The orbital velocity of such a planet at the periastron is 423.5 km s^{-1} . The velocity of the clumps in the outermost orbit is 389.5 km s^{-1} , corresponding to an orbital period of $P_{\text{orb}}^{\text{out}} = 128.5$ days. For the clumps in the innermost orbit, the velocity is 455.1 km s^{-1} , corresponding to an orbital period $P_{\text{orb}}^{\text{in}} = 80.6$ days. We can see that the difference of their orbital periods is 47.9 days. Below, we will consider the active windows of FRBs 180916 and 121102 in more detail.

The repetition period of FRB 180916 is 16.35 days and the active window is about 5 days. Figure 5 shows the period difference for the clumps in the innermost and outermost orbits as a function of the eccentricity and density. Under the partial disruption condition, a planet with $m = 10^{-5} M_{\odot}$ and $P_{\text{orb}} = 16.35$ days can produce clumps with period differences ranging from 4 to 6.25 days when the density ranges from $\bar{\rho} = 3 \text{ g cm}^{-3}$ to $\bar{\rho} = 10 \text{ g cm}^{-3}$. In these cases, the velocity of the planet is 429.7 km s^{-1} at the periastron. The velocity of the clumps in the outermost orbit is 406.4 km s^{-1} , corresponding to an orbital period $P_{\text{orb}}^{\text{out}} = 19$ days. For the clumps in the innermost orbit, the velocity is 451.9 km s^{-1} and the orbital period is $P_{\text{orb}}^{\text{in}} = 14$ days. The period difference is 5 days, which can satisfactorily meet the requirement of the observed active window of FRB 180916.

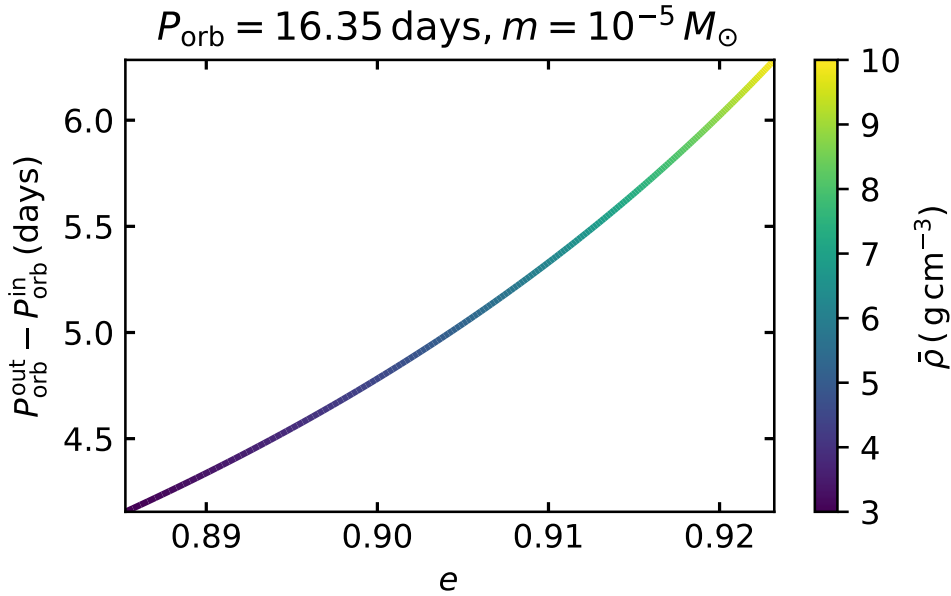


Figure 5. Difference of orbital periods for the clumps in the innermost and outermost orbits, plotted vs. the eccentricity for a planet in a 16.35 day orbit.

The repetition period of FRB 121102 is about 157 days, and the active window is ~ 87 days. Figure 6 shows the period difference for the clumps in the innermost and outermost orbit as a function of the eccentricity and density. Under the partial disruption condition, a planet with $m = 5 \times 10^{-7} M_{\odot}$ and $P_{\text{orb}} = 157$ days can produce clumps with period differences ranging from 65 days to about 105 days when the density ranges from $\bar{\rho} = 3 \text{ g cm}^{-3}$ to $\bar{\rho} = 10 \text{ g cm}^{-3}$. In these cases, the velocity of the planet is 437.57 km s^{-1} at periastron. The velocity of the clumps in the innermost orbit is 474.6 km s^{-1} , corresponding to an orbital period $P_{\text{orb}}^{\text{in}} = 123.06$ days. For the clumps in the outermost orbit, the velocity is 397.28 km s^{-1} and the orbital period is $P_{\text{orb}}^{\text{out}} = 209.78$ days. The period difference is 86.72 days. Again it can satisfactorily meet the requirement of the observed active window of FRB 121102.

Note that the gravitational perturbations from the planet itself still could influence the orbits of the clumps. Such perturbations can lead to changes in the inclination and eccentricity of the clump orbits so that the clumps will finally deviate from the line of sight. As a result, FRBs could be observed only from newly generated fragments, which maintains the periodicity and active window of the repeating FRBs. Below, we present more details on this issue.

In a triple system where a test particle revolves around its host in a close inner orbit while a third object moves around in an outer orbit, the eccentricity of the test particle can be significantly altered by the outer object. This is called the Kozai-Lidov effect, which can change the orbit of the test particle (Kozai 1962; Lidov 1962; Naoz 2016). In a normal Kozai-Lidov mechanism, the bigger planet’s orbit is usually assumed to be circular and the vertical angular momentum is conserved for the test particle. As a result, the eccentricity and inclination of the test particle’s orbit vary periodically. However, when the planet’s orbit is eccentric, the z-component of the inner and outer orbits’ angular momentum is not conserved, which leads to very different behaviors of the test particle (Lithwick & Naoz 2011; Li et al. 2014; Naoz et al. 2017). It was found that for a nearly coplanar (the inclination $i \sim 0$) and highly eccentric (for both inner and outer) configuration, the eccentricity of the test particle increases steadily, while the inclination i oscillates in a small range (Li et al. 2014). It was also found that, for a system with a tight-orbit configuration, the perturbation is strong and the orbit of the test particle can be altered on short timescales.

In our model, as mentioned above, the clumps coming from different parts of the planet move in slightly different orbits as compared with that of the planet. These orbits are approximately coplanar and close to each other. The surviving major portion of the planet can create perturbation. Unlike the case of Li et al. (2014), our system breaks the secular approximation condition. Such a case has been discussed by Antonini et al. (2014). They found that the inclination and eccentricity of the test object still could change in a short time. As a result, in our cases, the direction of the Alfvén wing and the FRB emission cone will deviate from our line of sight in a short time (e.g., after one or two orbital periods) due to the inclination change. No FRBs would be observed from older fragments.

To summarize, in our framework, the line of sight lies in the original orbital plane of the planet. The clumps generated during the partial disruption process near the periastron will pass through the observer’s line of sight one by one during their first round of motion in their new orbits, producing FRBs detectable by the observer. After that, the gravitational perturbation from the planet will change the orbits of the fragments so that they will no longer produce visible FRBs later. In other words, only new clumps generated near the periastron will produce FRBs. In this way, the periodicity and active window of the repeating FRBs can be well maintained.

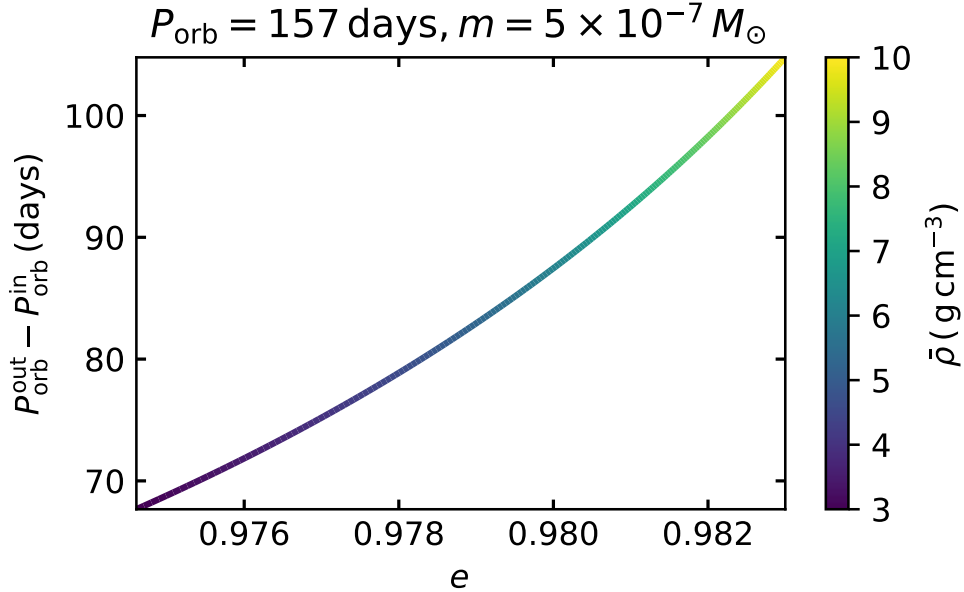


Figure 6. Difference of orbital periods for the clumps in the innermost and outermost orbits, plotted vs. the eccentricity for a planet in a 157 day orbit.

5. EVAPORATION TIMESCALE FOR AN OBJECT IN AN ECCENTRIC ORBIT

For a planet composed of ordinary matter orbiting around a pulsar, the evaporation timescale at a fixed distance is (Kotera et al. 2016)

$$t_{\text{ev}} = 7.2 \times 10^{-12} \text{yr} \left(\frac{R_c}{\text{km}} \right)^3 \left(\frac{\bar{\rho}}{\text{g cm}^{-3}} \right)^2 \left(\frac{r}{R_\odot} \right)^2 \frac{1}{L_{p,35} Q_{\text{abs}}}, \quad (11)$$

where $L_p = 9.6 \times 10^{34} \text{erg s}^{-1} I_{45} P_{\star,-3}^{-4} B_{\star,8}^2 R_{\star,6}^6$ is the spin-down luminosity of the pulsar (here the convention $Q_x = Q/10^x$ in cgs units is adopted), and Q_{abs} is the energy-absorption efficiency. Usually, $Q_{\text{abs}} = 3/N_r$ for large planets and $Q_{\text{abs}} = 12x/N_r^2 + 2x^3 N_r^2/15$ for small objects. Here, the refractive index is $N_r = \sqrt{\mu\sigma P_\star}$, with $\mu\sigma = 10^6 \text{s}^{-1}$ and the size ratio is defined as $x = R_c/cP_\star$. Taking $P_\star = 1 \text{s}$ and $B_\star = 10^{12} \text{G}$, the evaporation timescale is $t_{\text{ev}} \sim 10^4 \text{yr}$ for a small object with a density of $\bar{\rho} = 3 \text{g cm}^{-3}$ in a circular orbit of $r \sim 10^{11} \text{cm}$ (Kotera et al. 2016). However, the situation is very different for an object in a highly eccentric orbit, because the distance of the two objects varies in a very wide range. More importantly, for most of the time of each orbital cycle, the planet is far away from the pulsar. In our model, the periastron distance is $\sim 10^{11} \text{cm}$, but the average separation in one orbital period is much larger than this value. In the case of an elliptical orbit, the mean separation between the two objects is $\bar{r} = \frac{2}{P_{\text{orb}}} \int_0^{P_{\text{orb}}/2} r dt$ and can be calculated as

$$\bar{r} = \frac{a(1-e^2)^{5/2}}{\pi} \int_0^\pi \frac{1}{(1+e \cos \theta)^3} d\theta. \quad (12)$$

Substituting r in Eq. (11) with \bar{r} , we can estimate the evaporation timescale of a planet in an elliptical orbit. In our model, assuming $m = 10^{-5} M_\odot$, $P_{\text{orb}} = 16.35 \text{days}$, and $\bar{\rho} = 3 \text{g cm}^{-3}$, then the planet will be partially disrupted when $e = 0.88$. In this case, the evaporation timescale can be derived as $t_{\text{ev}} = 2 \times 10^7 \text{yr}$. If the mean density is taken as $\bar{\rho} = 10 \text{g cm}^{-3}$, then it will be partially disrupted when $e = 0.92$ and the evaporation timescale correspondingly becomes $t_{\text{ev}} = 7 \times 10^7 \text{yr}$. If we take the pulsar spin period as $P_\star = 1 \text{s}$, then we get $t_{\text{ev}} = 6.3 \times 10^{11} \text{yr}$ for $\bar{\rho} = 3 \text{g cm}^{-3}$, and $t_{\text{ev}} = 2.2 \times 10^{12} \text{yr}$ for $\bar{\rho} = 10 \text{g cm}^{-3}$. A planet with $m = 10^{-5} M_\odot$, $P_{\text{orb}} = 157 \text{days}$ and $\bar{\rho} = 3 \text{g cm}^{-3}$ will be partially disrupted when $e = 0.975$, corresponding to an evaporation timescale $t_{\text{ev}} = 4.6 \times 10^8 \text{yr}$. If the mean density is taken as $\bar{\rho} = 10 \text{g cm}^{-3}$, then it will be partially disrupted when $e = 0.983$, corresponding to an evaporation timescale $t_{\text{ev}} = 1.5 \times 10^9 \text{yr}$. If we change the pulsar spin period to $P_\star = 1 \text{s}$, then we get $t_{\text{ev}} = 1.6 \times 10^{13} \text{yr}$ for $\bar{\rho} = 3 \text{g cm}^{-3}$, and $t_{\text{ev}} = 4.9 \times 10^{13} \text{yr}$ for $\bar{\rho} = 10 \text{g cm}^{-3}$. From the above calculations, we can see that the evaporation timescale of a planet in our elliptical orbit is generally very large. Therefore, the effect of evaporation is negligible in this framework.

6. FORMATION OF HIGH-ECCENTRICITY PLANETARY SYSTEMS

In Section 3, we demonstrated that to account for the observed repeating FRB periods ranging from tens of days to over one hundred days, a highly elliptical planet orbit with $e \geq 0.9$ is needed. It is a natural question that whether such highly elliptical orbits are possible or not for planets. Here we present some discussion on this issue.

Since the discovery of the first extrasolar planet around PSR 1257+12 (Wolszczan & Frail 1992), about 4700 exoplanets (as of 2021 April 27) have been discovered (see Extrasolar Planets Encyclopaedia – EU ¹; (Schneider et al. 2011)). Among them, more than 10 objects are pulsar planet candidates. Although the eccentricities of these pulsar planet candidates are generally very small, high-eccentricity pulsar binaries have been discovered (see references in the databases “Pulsars in globular clusters” ² and The ATNF pulsar catalog ³; (Manchester et al. 2005)). Additionally, a few planets with a large eccentricity orbiting around other types of stars have also been detected (see the EU database). Good examples for these include HD 20782 b ($e = 0.97 \pm 0.01$), HD 80606 b ($e = 0.93366 \pm 0.00043$), HD 7449 A b ($e = 0.92 \pm 0.03$), and HD 4113 A b ($e = 0.903 \pm 0.005$). The existence of these special planets indicates that the formation of high-eccentricity planetary systems around compact objects should also be possible. Planets with a large eccentricity could be formed around a NS through at least three channels. First, a free-floating planet (FFP) can be captured by a NS when they are in a close encounter. Second, exchange/snatch of a planet may happen between a NS and a nearby main-sequence planetary system. Thirdly, the Kozai-Lidov effect in a multibody system may give birth to a high-eccentricity planet. Below, we discuss these three processes briefly.

- Formation from the capture of FFPs by NS:

FFPs are common in space (Smith & Bonnell 2001; Hurley & Shara 2002; Sumi et al. 2011; van Elteren et al. 2019; Johnson et al. 2020; Mróz et al. 2020). They may be formed from various dynamical interactions (see

¹ <http://www.exoplanet.eu/>

² <http://www.naic.edu/~pfreire/GCpsr.html>

³ <https://www.atnf.csiro.au/research/pulsar/psrcat/>

Figure 1 in Kremer et al. (2019)), such as ejection from dying multiple-star systems (Veras & Tout 2012; Wang et al. 2015; van Elteren et al. 2019), planet-planet scattering (Hong et al. 2018; van Elteren et al. 2019), or the encounter of a star with other planetary systems (Hurley & Shara 2002). In a cluster’s full lifetime, about 10% — 50% of primordial planetary systems experience various dynamical encounters and many planets become FFPs. About 30% — 80% of them escape the cluster due to strong dynamical encounters and/or tidal interactions (Kremer et al. 2019) and travel freely in space. The velocity of these FFPs is typically in the range of 0 — 30 km s⁻¹ (Smith & Bonnell 2001; Hurley & Shara 2002). FFPs may be captured by other stars or planetary systems and form highly eccentric planetary systems (Parker & Quanz 2012; Wang et al. 2015; Li & Adams 2016; Gouliniski & Ribak 2018; Hands et al. 2019; van Elteren et al. 2019). A simulation by Gouliniski & Ribak (2018) showed that more than 99.1% of the captured planets are in an orbit with $e > 0.85$, and the masses of FFPs do not affect the eccentricity significantly.

- Formation from NS exchange/snatch a planet:

Pulsars can obtain a kick velocity when they are born in the supernova explosion. If a planet survives in supernova, the newborn high-speed pulsar and the surviving planet may form an eccentric planetary system by gravitational interaction. Additionally, when a pulsar moves with a kick velocity of 100 — 400 km s⁻¹ in space, it may pass by a planetary system. During this process, the pulsar can also exchange/snatch a planet from other planetary systems via gravitational perturbations. Planetary systems formed in this way may also be eccentric.

- Formation from the Kozai-Lidov effect in a multibody system:

The Kozai-Lidov effect (Kozai 1962; Lidov 1962; Naoz 2016) can explain the dynamics of multibody systems in which one companion in an outer orbit can change (increase) the eccentricity of objects in inner orbits by gravitational perturbations. The timescale for forming a high-eccentricity system is determined by the initial parameters. If the central star of such a multibody system is a NS then a highly eccentric NS-planet system may form.

From the above descriptions, we can see that there are many routes to form high-eccentricity planets around NSs. The requirement of $e \geq 0.9$ in our framework thus in principle can be met in reality.

Here, we roughly calculate the population of highly eccentric planetary systems in the Milky Way. It is estimated that there are 100 – 400 billion stars in our Galaxy (see the Universe Today⁴ and NASA⁵ websites). A study based on the microlensing observations suggests that each star hosts 1.6 planets on average (Cassan et al. 2012). Taking 200 billion as the rough number of stars, then there would be about 320 billion planets in the Milky Way. Since about 10% — 50% of primordial planetary systems experience various dynamical encounters and produce FFPs as mentioned above (Kremer et al. 2019), it is expected that there should be 20 – 100 billion FFPs in the whole Galaxy. More than 85% of the stars in the Galactic disk are in a mass range of $0.1M_{\odot} < M < 2M_{\odot}$. About 1% of them are expected to experience at least one capture process during their lifetime (Gouliniski & Ribak 2018). This allows us to estimate that there are 1.7 billion captures and 99.1% (1.68 billion) of them give birth to planets in a highly eccentric orbit with $e > 0.85$. Currently, four highly eccentric ($e > 0.9$) planets have been confirmed among the observed 4700 planets, corresponding to a fraction of 0.085%. Using this ratio as a reference, it can be estimated that the number of highly eccentric ($e > 0.9$) planetary systems in our Galaxy is ~ 170 million. From the above analysis, we can see that highly eccentric planetary systems are copious in the Milky Way. However, it is not easy to detect them due to various observational biases. For these planets, the evaporation again can be safely omitted since the timescale is usually much more than 10^7 yr.

7. CONCLUSIONS AND DISCUSSION

In this study, we aimed to explain the periodic repeatability of FRBs by considering a NS-planet interaction model. In our framework, a planet moves around its host NS in a highly eccentric orbit. The periastron of the planet satisfies a special condition $r_{\text{td}} \leq r_{\text{p}} \leq 2r_{\text{td}}$, so that the crust of the planet will be partially disrupted every time it pass through the periastron. Fragments of the size of a few kilometers are produced in the process. During the process, the fragments interact with the pulsar wind via the Alfvén wing mechanism to give birth to FRBs. The periods of

⁴ <https://www.universetoday.com/30296/how-many-planets-are-in-the-galaxy/>

⁵ <https://asd.gsfc.nasa.gov/blueshift/index.php/2015/07/22/how-many-stars-in-the-milky-way/>

repeating FRBs correspond to the orbit periods of the planets. To account for the observed period of $\sim 10 - 100$ days, an orbital eccentricity larger than ~ 0.9 is generally required. It is shown that the basic features of the two well-known repeating sources, FRBs 121102 and 180916, can be satisfactorily interpreted by the model.

It is interesting to note that the interaction of small bodies with NSs has already been studied to interpret repeating FRBs, but generally in a very different framework. For example, Dai et al. (2016) explained repeating FRBs as due to the multiple collisions that happen when a NS travels through an asteroid belt. Decoene et al. (2021) even suggested a three-component scenario which involves a NS, an asteroid belt around it, and a third outer companion. In their model, the outer companion can be a black hole, a NS, a WD or a main-sequence star. While our model is in principle different, we would like to point out that some ingredients in the above models may also play a role in our model. For example, when the fragments finally arrive at the NS and collide with it, FRBs may be produced via the NS-asteroid collision mechanism (Geng & Huang 2015; Dai et al. 2016). Yet, the time needed for the clumps to fall into the NS is highly uncertain and still needs to be further studied. Note that the disruption distance of rocky planets is $\sim 10^{11}$ cm (Mottez et al. 2013a,b). At this distance, the evaporation takes a time of only $\sim 10^4$ yr (Kotera et al. 2016). However, the ellipticity of the orbit can prolong the evaporation timescale by several orders of magnitude, to $\geq 10^7$ yr. Therefore, the evaporation does not affect our model significantly.

8. ACKNOWLEDGMENTS

We would like to thank the anonymous referee for helpful suggestions that led to significant improvement of our study. This work is supported by the special research assistance project of the Chinese Academy of Sciences (CAS), by the National Natural Science Foundation of China (grant Nos. 12041306, 12041304, 11873030, U1938201, U1838113, U2031209, 11903019, 11833003, 12033001, 12103055), by the National Key R&D Program of China (grant No. 2021YFA0718500), by the National SKA Program of China (grant No. 2020SKA0120300), by the CAS ‘‘Light of West China’’ Program (grant No. 2018-XBQNXZ-B-025), by the science research grants from the China Manned Space Project with No. CMS-CSST-2021-B11, and by the Operation, Maintenance and Upgrading Fund for Astronomical Telescopes and Facility Instruments, budgeted from the Ministry of Finance of China (MOF) and administrated by the CAS. This work is also partially supported by the Strategic Priority Research Program of the CAS under grant No. XDA15360300.

Software: SciPy (Virtanen et al. 2020), Matplotlib (Hunter 2007), NumPy (van der Walt et al. 2011) .

REFERENCES

- Antonini, F., Murray, N., & Mikkola, S. 2014, ApJ, 781, 45, doi: [10.1088/0004-637X/781/1/45](https://doi.org/10.1088/0004-637X/781/1/45)
- Bear, E., & Soker, N. 2013, NewA, 19, 56, doi: [10.1016/j.newast.2012.08.004](https://doi.org/10.1016/j.newast.2012.08.004)
- Brook, P. R., Karastergiou, A., Buchner, S., et al. 2014, ApJL, 780, L31, doi: [10.1088/2041-8205/780/2/L31](https://doi.org/10.1088/2041-8205/780/2/L31)
- Campana, S., Lodato, G., D’Avanzo, P., et al. 2011, Nature, 480, 69, doi: [10.1038/nature10592](https://doi.org/10.1038/nature10592)
- Cassan, A., Kubas, D., Beaulieu, J. P., et al. 2012, Nature, 481, 167, doi: [10.1038/nature10684](https://doi.org/10.1038/nature10684)
- Chime/Frb Collaboration, Amiri, M., Andersen, B. C., et al. 2020, Nature, 582, 351, doi: [10.1038/s41586-020-2398-2](https://doi.org/10.1038/s41586-020-2398-2)
- Cordes, J. M., & Chatterjee, S. 2019, ARA&A, 57, 417, doi: [10.1146/annurev-astro-091918-104501](https://doi.org/10.1146/annurev-astro-091918-104501)
- Cordes, J. M., & Shannon, R. M. 2008, ApJ, 682, 1152, doi: [10.1086/589425](https://doi.org/10.1086/589425)
- Dai, Z. G. 2020, ApJL, 897, L40, doi: [10.3847/2041-8213/aba11b](https://doi.org/10.3847/2041-8213/aba11b)
- Dai, Z. G., Wang, J. S., Wu, X. F., & Huang, Y. F. 2016, ApJ, 829, 27, doi: [10.3847/0004-637X/829/1/27](https://doi.org/10.3847/0004-637X/829/1/27)
- Dai, Z. G., & Zhong, S. Q. 2020, ApJL, 895, L1, doi: [10.3847/2041-8213/ab8f2d](https://doi.org/10.3847/2041-8213/ab8f2d)
- Decoene, V., Kotera, K., & Silk, J. 2021, A&A, 645, A122, doi: [10.1051/0004-6361/202038975](https://doi.org/10.1051/0004-6361/202038975)
- Du, S., Wang, W., Wu, X., & Xu, R. 2021, MNRAS, 500, 4678, doi: [10.1093/mnras/staa3527](https://doi.org/10.1093/mnras/staa3527)
- Geng, J., Li, B., & Huang, Y. 2021, The Innovation, 2, 100152, doi: [10.1016/j.xinn.2021.100152](https://doi.org/10.1016/j.xinn.2021.100152)
- Geng, J. J., & Huang, Y. F. 2015, ApJ, 809, 24, doi: [10.1088/0004-637X/809/1/24](https://doi.org/10.1088/0004-637X/809/1/24)
- Geng, J.-J., Li, B., Li, L.-B., et al. 2020, ApJL, 898, L55, doi: [10.3847/2041-8213/aba83c](https://doi.org/10.3847/2041-8213/aba83c)
- Gouliniski, N., & Ribak, E. N. 2018, MNRAS, 473, 1589, doi: [10.1093/mnras/stx2506](https://doi.org/10.1093/mnras/stx2506)
- Granvik, M., Morbidelli, A., Jedicke, R., et al. 2016, Nature, 530, 303, doi: [10.1038/nature16934](https://doi.org/10.1038/nature16934)
- Gu, W.-M., Dong, Y.-Z., Liu, T., Ma, R., & Wang, J. 2016, ApJL, 823, L28, doi: [10.3847/2041-8205/823/2/L28](https://doi.org/10.3847/2041-8205/823/2/L28)

- Gu, W.-M., Yi, T., & Liu, T. 2020, *MNRAS*, 497, 1543, doi: [10.1093/mnras/staa1914](https://doi.org/10.1093/mnras/staa1914)
- Hands, T. O., Dehnen, W., Gration, A., Stadel, J., & Moore, B. 2019, *MNRAS*, 490, 21, doi: [10.1093/mnras/stz1069](https://doi.org/10.1093/mnras/stz1069)
- Hills, J. G. 1975, *Nature*, 254, 295, doi: [10.1038/254295a0](https://doi.org/10.1038/254295a0)
- Hong, Y.-C., Raymond, S. N., Nicholson, P. D., & Lunine, J. I. 2018, *ApJ*, 852, 85, doi: [10.3847/1538-4357/aaa0db](https://doi.org/10.3847/1538-4357/aaa0db)
- Huang, Y. F., & Geng, J. J. 2014, *ApJL*, 782, L20, doi: [10.1088/2041-8205/782/2/L20](https://doi.org/10.1088/2041-8205/782/2/L20)
- Huang, Y. F., & Yu, Y. B. 2017, *ApJ*, 848, 115, doi: [10.3847/1538-4357/aa8b63](https://doi.org/10.3847/1538-4357/aa8b63)
- Hunter, J. D. 2007, *Computing in Science and Engineering*, 9, 90, doi: [10.1109/MCSE.2007.55](https://doi.org/10.1109/MCSE.2007.55)
- Hurley, J. R., & Shara, M. M. 2002, *ApJ*, 565, 1251, doi: [10.1086/337921](https://doi.org/10.1086/337921)
- Ioka, K., & Zhang, B. 2020, *ApJL*, 893, L26, doi: [10.3847/2041-8213/ab83fb](https://doi.org/10.3847/2041-8213/ab83fb)
- Johnson, S. A., Penny, M., Gaudi, B. S., et al. 2020, *The Astronomical Journal*, 160, 123, doi: [10.3847/1538-3881/aba75b](https://doi.org/10.3847/1538-3881/aba75b)
- Katz, J. I. 2018, *Progress in Particle and Nuclear Physics*, 103, 1, doi: [10.1016/j.pnpnp.2018.07.001](https://doi.org/10.1016/j.pnpnp.2018.07.001)
- Keane, E. F., Stappers, B. W., Kramer, M., & Lyne, A. G. 2012, *MNRAS*, 425, L71, doi: [10.1111/j.1745-3933.2012.01306.x](https://doi.org/10.1111/j.1745-3933.2012.01306.x)
- Kotera, K., Mottez, F., Voisin, G., & Heyvaerts, J. 2016, *A&A*, 592, A52, doi: [10.1051/0004-6361/201628116](https://doi.org/10.1051/0004-6361/201628116)
- Kozai, Y. 1962, *AJ*, 67, 591, doi: [10.1086/108790](https://doi.org/10.1086/108790)
- Kremer, K., D’Orazio, D. J., Samsing, J., Chatterjee, S., & Rasio, F. A. 2019, *ApJ*, 885, 2, doi: [10.3847/1538-4357/ab44d1](https://doi.org/10.3847/1538-4357/ab44d1)
- Kuerban, A., Geng, J.-J., Huang, Y.-F., Zong, H.-S., & Gong, H. 2020, *ApJ*, 890, 41, doi: [10.3847/1538-4357/ab698b](https://doi.org/10.3847/1538-4357/ab698b)
- Levin, Y., Beloborodov, A. M., & Bransgrove, A. 2020, *ApJL*, 895, L30, doi: [10.3847/2041-8213/ab8c4c](https://doi.org/10.3847/2041-8213/ab8c4c)
- Li, G., & Adams, F. C. 2016, *ApJL*, 823, L3, doi: [10.3847/2041-8205/823/1/L3](https://doi.org/10.3847/2041-8205/823/1/L3)
- Li, G., Naoz, S., Kocsis, B., & Loeb, A. 2014, *ApJ*, 785, 116, doi: [10.1088/0004-637X/785/2/116](https://doi.org/10.1088/0004-637X/785/2/116)
- Lidov, M. L. 1962, *Planetary and Space Science*, 9, 719, doi: [10.1016/0032-0633\(62\)90129-0](https://doi.org/10.1016/0032-0633(62)90129-0)
- Lithwick, Y., & Naoz, S. 2011, *ApJ*, 742, 94, doi: [10.1088/0004-637X/742/2/94](https://doi.org/10.1088/0004-637X/742/2/94)
- Liu, S.-F., Guillochon, J., Lin, D. N. C., & Ramirez-Ruiz, E. 2013, *ApJ*, 762, 37, doi: [10.1088/0004-637X/762/1/37](https://doi.org/10.1088/0004-637X/762/1/37)
- Lorimer, D. R., Bailes, M., McLaughlin, M. A., Narkevic, D. J., & Crawford, F. 2007, *Science*, 318, 777, doi: [10.1126/science.1147532](https://doi.org/10.1126/science.1147532)
- Lyutikov, M., Barkov, M. V., & Giannios, D. 2020, *ApJL*, 893, L39, doi: [10.3847/2041-8213/ab87a4](https://doi.org/10.3847/2041-8213/ab87a4)
- Malamud, U., & Perets, H. B. 2020a, *MNRAS*, 492, 5561, doi: [10.1093/mnras/staa142](https://doi.org/10.1093/mnras/staa142)
- . 2020b, *MNRAS*, 493, 698, doi: [10.1093/mnras/staa143](https://doi.org/10.1093/mnras/staa143)
- Manchester, R. N., Hobbs, G. B., Teoh, A., & Hobbs, M. 2005, *AJ*, 129, 1993, doi: [10.1086/428488](https://doi.org/10.1086/428488)
- Manser, C. J., Gänsicke, B. T., Eggl, S., et al. 2019, *Science*, 364, 66, doi: [10.1126/science.aat5330](https://doi.org/10.1126/science.aat5330)
- Mottez, F., Bonazzola, S., & Heyvaerts, J. 2013a, *A&A*, 555, A125, doi: [10.1051/0004-6361/201321182](https://doi.org/10.1051/0004-6361/201321182)
- . 2013b, *A&A*, 555, A126, doi: [10.1051/0004-6361/201321184](https://doi.org/10.1051/0004-6361/201321184)
- Mottez, F., & Heyvaerts, J. 2020, *A&A*, 639, C2, doi: [10.1051/0004-6361/201116530e](https://doi.org/10.1051/0004-6361/201116530e)
- Mottez, F., & Zarka, P. 2014, *A&A*, 569, A86, doi: [10.1051/0004-6361/201424104](https://doi.org/10.1051/0004-6361/201424104)
- Mottez, F., Zarka, P., & Voisin, G. 2020, *A&A*, 644, A145, doi: [10.1051/0004-6361/202037751](https://doi.org/10.1051/0004-6361/202037751)
- Mróz, P., Poleski, R., Gould, A., et al. 2020, *ApJL*, 903, L11, doi: [10.3847/2041-8213/abbfad](https://doi.org/10.3847/2041-8213/abbfad)
- Naoz, S. 2016, *ARA&A*, 54, 441, doi: [10.1146/annurev-astro-081915-023315](https://doi.org/10.1146/annurev-astro-081915-023315)
- Naoz, S., Li, G., Zanardi, M., de Elía, G. C., & Di Sisto, R. P. 2017, *AJ*, 154, 18, doi: [10.3847/1538-3881/aa6fb0](https://doi.org/10.3847/1538-3881/aa6fb0)
- Parker, R. J., & Quanz, S. P. 2012, *MNRAS*, 419, 2448, doi: [10.1111/j.1365-2966.2011.19911.x](https://doi.org/10.1111/j.1365-2966.2011.19911.x)
- Petroff, E., Hessels, J. W. T., & Lorimer, D. R. 2019, *A&A Rv*, 27, 4, doi: [10.1007/s00159-019-0116-6](https://doi.org/10.1007/s00159-019-0116-6)
- Petroff, E., Johnston, S., Keane, E. F., et al. 2015, *MNRAS*, 454, 457, doi: [10.1093/mnras/stv1953](https://doi.org/10.1093/mnras/stv1953)
- Platts, E., Weltman, A., Walters, A., et al. 2019, *PhR*, 821, 1, doi: [10.1016/j.physrep.2019.06.003](https://doi.org/10.1016/j.physrep.2019.06.003)
- Rajwade, K. M., Mickaliger, M. B., Stappers, B. W., et al. 2020, *MNRAS*, 495, 3551, doi: [10.1093/mnras/staa1237](https://doi.org/10.1093/mnras/staa1237)
- Schneider, J., Dedieu, C., Le Sidaner, P., Savalle, R., & Zolotukhin, I. 2011, *A&A*, 532, A79, doi: [10.1051/0004-6361/201116713](https://doi.org/10.1051/0004-6361/201116713)
- Sepinsky, J. F., Willems, B., & Kalogera, V. 2007, *ApJ*, 660, 1624, doi: [10.1086/513736](https://doi.org/10.1086/513736)
- Smallwood, J. L., Martin, R. G., & Zhang, B. 2019, *MNRAS*, 485, 1367, doi: [10.1093/mnras/stz483](https://doi.org/10.1093/mnras/stz483)
- Smith, K. W., & Bonnell, I. A. 2001, *MNRAS*, 322, L1, doi: [10.1046/j.1365-8711.2001.04321.x](https://doi.org/10.1046/j.1365-8711.2001.04321.x)
- Sob’yanin, D. N. 2020, *MNRAS*, 497, 1001, doi: [10.1093/mnras/staa1976](https://doi.org/10.1093/mnras/staa1976)
- Stephan, A. P., Naoz, S., & Zuckerman, B. 2017, *ApJL*, 844, L16, doi: [10.3847/2041-8213/aa7cf3](https://doi.org/10.3847/2041-8213/aa7cf3)
- Sumi, T., Kamiya, K., Bennett, D. P., et al. 2011, *Nature*, 473, 349, doi: [10.1038/nature10092](https://doi.org/10.1038/nature10092)

- Thornton, D., Stappers, B., Bailes, M., et al. 2013, *Science*, 341, 53, doi: [10.1126/science.1236789](https://doi.org/10.1126/science.1236789)
- van der Walt, S., Colbert, S. C., & Varoquaux, G. 2011, *Computing in Science and Engineering*, 13, 22, doi: [10.1109/MCSE.2011.37](https://doi.org/10.1109/MCSE.2011.37)
- van Elteren, A., Portegies Zwart, S., Pelupessy, I., Cai, M. X., & McMillan, S. L. W. 2019, *A&A*, 624, A120, doi: [10.1051/0004-6361/201834641](https://doi.org/10.1051/0004-6361/201834641)
- Vanderburg, A., Johnson, J. A., Rappaport, S., et al. 2015, *Nature*, 526, 546, doi: [10.1038/nature15527](https://doi.org/10.1038/nature15527)
- Veras, D., & Tout, C. A. 2012, *MNRAS*, 422, 1648, doi: [10.1111/j.1365-2966.2012.20741.x](https://doi.org/10.1111/j.1365-2966.2012.20741.x)
- Virtanen, P., Gommers, R., Oliphant, T. E., et al. 2020, *Nature Methods*, 17, 261, doi: [10.1038/s41592-019-0686-2](https://doi.org/10.1038/s41592-019-0686-2)
- Voisin, G., Mottez, F., & Zarka, P. 2021, *MNRAS*, 508, 2079, doi: [10.1093/mnras/stab2622](https://doi.org/10.1093/mnras/stab2622)
- Wang, L., Kouwenhoven, M. B. N., Zheng, X., Church, R. P., & Davies, M. B. 2015, *MNRAS*, 449, 3543, doi: [10.1093/mnras/stv542](https://doi.org/10.1093/mnras/stv542)
- Wolszczan, A., & Frail, D. A. 1992, *Nature*, 355, 145, doi: [10.1038/355145a0](https://doi.org/10.1038/355145a0)
- Xiao, D., Wang, F., & Dai, Z. 2021, *Science China Physics, Mechanics, and Astronomy*, 64, 249501, doi: [10.1007/s11433-020-1661-7](https://doi.org/10.1007/s11433-020-1661-7)
- Yang, H., & Zou, Y.-C. 2020, *ApJL*, 893, L31, doi: [10.3847/2041-8213/ab800f](https://doi.org/10.3847/2041-8213/ab800f)
- Yang, Y.-P. 2021, *ApJ*, 920, 34, doi: [10.3847/1538-4357/ac2146](https://doi.org/10.3847/1538-4357/ac2146)
- Yang, Y.-P., & Zhang, B. 2021, *ApJ*, 919, 89, doi: [10.3847/1538-4357/ac14b5](https://doi.org/10.3847/1538-4357/ac14b5)
- Yu, Y.-B., & Huang, Y.-F. 2016, *Research in Astronomy and Astrophysics*, 16, 75, doi: [10.1088/1674-4527/16/5/075](https://doi.org/10.1088/1674-4527/16/5/075)
- Zanazzi, J. J., & Lai, D. 2020, *ApJL*, 892, L15, doi: [10.3847/2041-8213/ab7cdd](https://doi.org/10.3847/2041-8213/ab7cdd)
- Zarka, P. 2007, *Planet. Space Sci.*, 55, 598, doi: [10.1016/j.pss.2006.05.045](https://doi.org/10.1016/j.pss.2006.05.045)
- Zarka, P., Treumann, R. A., Ryabov, B. P., & Ryabov, V. B. 2001, *Ap&SS*, 277, 293, doi: [10.1023/A:1012221527425](https://doi.org/10.1023/A:1012221527425)
- Zhang, B. 2017, *ApJL*, 836, L32, doi: [10.3847/2041-8213/aa5ded](https://doi.org/10.3847/2041-8213/aa5ded)
- . 2018, *ApJL*, 854, L21, doi: [10.3847/2041-8213/aaadba](https://doi.org/10.3847/2041-8213/aaadba)
- . 2020, *Nature*, 587, 45, doi: [10.1038/s41586-020-2828-1](https://doi.org/10.1038/s41586-020-2828-1)